Korean J. Chem. Eng., 37(9), 1466-1481 (2020)
DOI: 10.1007/s11814-020-0566-6

pISSN: 0256-1115
eISSN: 1975-7220

Experimental study on thermo-hydraulic performance of nanofluids in diverse axial ratio elliptical tubes with a built-in turbulator

Cong Qi*,,†, Tiantian Chen*,**, Yuxing Wang*,**, and Liyuan Yang*,****

*Jiangsu Province Engineering Laboratory of High Efficient Energy Storage Technology and Equipment, China University of Mining and Technology, Xuzhou 221116, China
**School of Electrical and Power Engineering, China University of Mining and Technology, Xuzhou 221116, China
(*Received 21 February 2020 • Revised 17 April 2020 • Accepted 30 April 2020*)

Abstract−Due to the low heat transfer efficiency of common heat exchange systems, an improved heat exchange system was developed. Enhanced tubes (elliptical tubes with a built-in turbulator) instead of a smooth tube were used and TiO_2-water nanofluids were substituted for water to intensify the heat transfer. The influences of turbulator (presence or absence), axial ratios of elliptical tubes (Z=1.235, 1.471, 1.706), nanoparticle concentration (ω=0.0 wt%, 0.1 wt%, 0.3 wt%, 0.5 wt%), and Reynolds number (Re=400-12,000) on the flow and heat transfer properties of TiO_2-water nanofluids were studied. Thermal and exergy efficiency were used to research the comprehensive thermo-hydraulic characteristics of these heat transfer enhancement technologies. The thermo-hydraulic properties of nanofluids all showed an increasing trend with the growing axial ratio, nanoparticle concentration and Reynolds number. Nanofluids (ω=0.5 wt%) in an elliptical tube (Z=1.706) with a built-in turbulator showed the best thermal performance, which could be increased by 33.8% in comparison with water at best. The thermal efficiency index increased first and then decreased with the Re. Nanofluids in elliptical tubes with a built-in turbulator can clearly promote heat transfer under the identical condition.

Keywords: Nanofluids, Forced Convection, Elliptical Tube, Thermal Efficiency, Exergy Efficiency

INTRODUCTION

Enhanced heat transfer technologies mainly contain two kinds: active reinforcement technique, which requires the consumption of additional energy, and passive reinforcement technique (such as pulsating heat pipe [1,2]). This paper mainly focuses on the latter. Passive reinforcement techniques mainly are improving the heat transfer surface and using a high heat conductivity heat transfer medium. An elliptical tube, as a common and effective enhanced tube, is used to substitute for the glossy tube in heat exchange systems. For heat transfer medium, nanofluids, as a high heat conductivity heat transfer medium [3,4], are applied in numerous areas, for instance, photo-thermal conversion based on various nanofluids including photonic nanofluids [5] and plasmonic nanoshell-based nanofluids [6], thermal and energy management application [7-9], and so on. Nanofluids are a proper effective heat transfer medium that can be applied in the heat transfer system instead of conventional fluids such as water.

Many studies have been conducted on the free convection of nanofluids in an oblique cavity [10], a lid-driven cavity [11], an open cavity [12], a rotating chamber [13], a cavity with a corrugated partition [14], a square cavity [15], a porous media [16], and a Γ-shaped enclosure [17]. Free convection shows the advantage of safe and silence, but it is only suitable for the fields with low heat transfer intensity requirements. For the high heat transfer intensity field, especially the heat exchanger system, the turbulent flow is widely adopted instead of the natural convection to achieve high-intensity heat transfer.

Turbulent flow heat transfer, as a main heat transfer model, is of great significance in the design of the heat exchange system. Numerous researches on the turbulent flow of nanofluids are being carried out. Hu et al. [18] conducted a numerical simulation on the turbulent flow of salt-based nanofluids among the solar energy system. Results indicated that the heat transmission characteristic of salt-based nanofluids firstly increases with nanoparticle concentration and then decreases, and the crucial concentration of nanoparticle is 1.0 wt%. Li et al. conducted a number of studies about the turbulent flow of nanofluids [19,20] in cavities [21-23], a pipe with modified turbulators [24], and a round duct with volute turbulators [25]. It was presented that the magnetic field, porous media, and turbulator play a positive part in improving heat transmission. Al-Rashed et al. [26,27] and Alsarraf et al. [28] considered the turbulent flow in a heat exchanger, discussed the influences of nanoparticle shapes, respectively [27,28], and analyzed the entropy generation [27]. It was determined that a platelet shaped nanoparticle shows the highest thermal performance, and high nanoparticle concentration can cause large entropy generation. Nojoomizadeh et al. [29] investigated the turbulent flow of nanofluids in a microchannel with the lower section filled with porous media, and concluded that decreasing permeability can cause high thermal performance at the upper section of the microchannel and low thermal performance at the lower section. Naphon et al. [30] investigated the tur-

†To whom correspondence should be addressed.
E-mail: qicong@cumt.edu.cn

bulent flow in a microchannel heat sink, and results presented that high nanoparticle concentration and low nozzle diameter are beneficial to the thermal performance. Sajid et al. [31] reviewed the application of nanofluids from the perspective of turbulent flow. Many studies on the nanofluid turbulent flow in a heat sink [32], a rectangular microchannel [33], a compact heat exchanger [34], a square channel [35], a pipe [36] have been conducted. It was found that nanofluids show an excellent characteristic compared with water.

In addition to the above excellent thermal-property heat transfer mediums, numerous researches on the turbulent flow of enhanced tubes are also investigated. Mohebbi et al. [37] revealed the turbulent flow performance of nanofluids in a costate channel. Results showed that the high ratio of block height can cause large thermal performance. Sun et al. [38] and Karimi [39] performed researches on the turbulent flow of nanofluids in a threaded tube with a built-in crooked belt and a double tube heat exchanger with a built-in tape, respectively. It was shown that the built-in crooked belt can cause a great improvement in thermal behavior. Naphon et al. implemented investigations on the turbulent flow of nanofluids in enhanced tubes, for instance, a micro-fin tube [40], a spirally corrugated tube [41], and a coiled tube [42]. Qi et al. also conducted feasible experiments studying the turbulent flow of nanofluids in enhanced tubes, for example, triangular tube [43]. All above enhanced tubes have merits of high thermal performance and are widely used in heat exchange systems.

From the above studies, the turbulent flow of nanofluids has been widely investigated, and diverse kinds of enhanced tubes were also investigated, which makes an outstanding contribution to the heat exchange system. However, the influence of enhanced tube structure, especially the elliptical tube with built-in turbulator, on the thermo-hydraulic characteristics of nanofluids in the heat exchange system is less researched. Hence, the effects of the elliptical tube structure were experimentally researched in this study. The innovations of the paper are mainly: (1) Effects of the coupling of elliptical tube structures (diverse axial ratios) and built-in turbulators are analyzed. (2) A comprehensive method (thermal efficiency) is adopted to evaluate the heat transfer and flow, which is helpful for the design and operation of the thermal system.

METHOD

1. Heat Medium

In this experimental system, the heat transfer media were TiO_2-water nanofluids with various concentrations (ω=0.0 wt%, 0.1 wt%, 0.3 wt%, 0.5 wt%). A two-step method was adopted to make preparation. The details of preparation step: A set amount of the dispersant was poured into deionized water and mechanically stirred for one hour; the nanoparticles were added slowly into the solution, and then the mixed suspension was placed on a magnetic stirrer for 40 minutes; the pH of the solution wasadjusted to 8 (researches of [43] showed that TiO_2-water nanofluids have the optimal stability when the pH=8); finally, it was oscillated in an ultrasonic oscillator for 40 minutes. Thermal physical parameters (heat conductivity and viscosity) are given in Table 1.

2. System

The experimental system adopted was one identical to our previous published paper, which is shown in Fig. 1 [44], where the details of the experimental system can also be found. However, only one kind of elliptical tube without a built-in turbulator was investigated in our previous paper [44]. For the sake of further investigating the effects of various elliptical tube structures with a built-in

Table 1. Physical parameters of nanoparticle and deionized water

Physical parameters	ρ (kg·m^{-3})	μ (Pa·s)	k (W·m^{-1}·K^{-1})
Deionized water	997.1	0.001004	0.6130
TiO_2	4250	-	8.9538

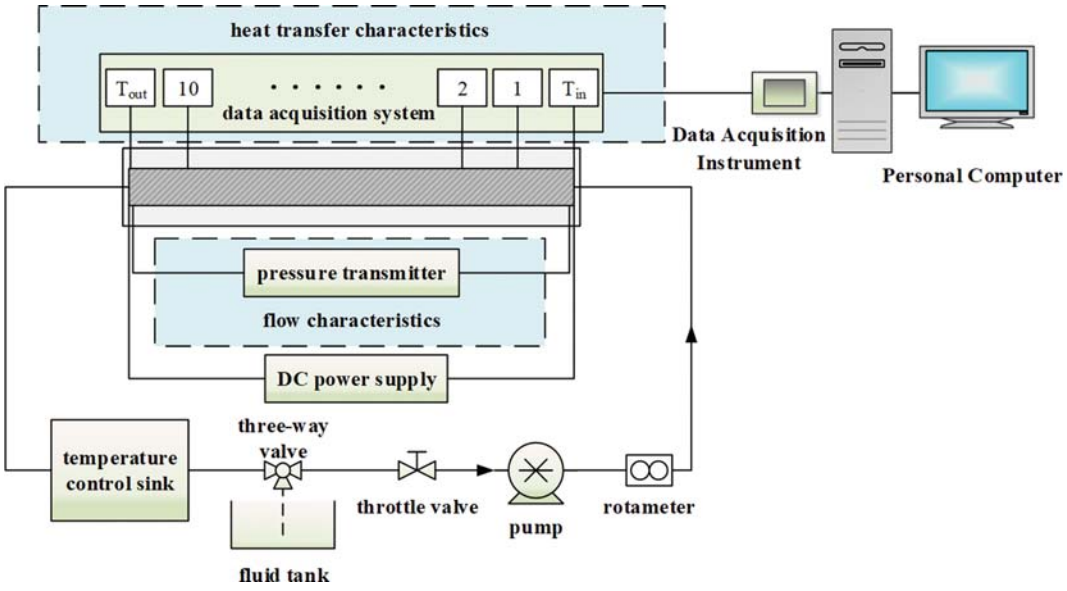

Fig. 1. Schematic plan of test system of nanofluids [44].

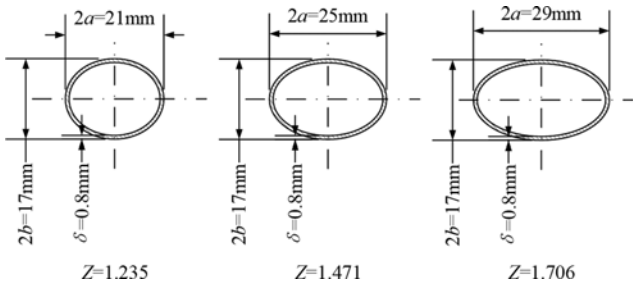

Fig. 2. Schematic plan of the elliptical tube.

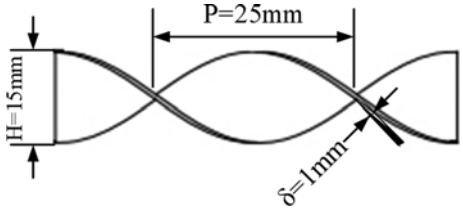

Fig. 3. Particulars of turbulator.

turbulator, three various types of elliptical tubes with a built-in turbulator were chosen to be the heat transfer tubes. The details of three various types of elliptical tubes are indicated in Fig. 2 and the turbulator is presented in Fig. 3. The axial ratios of these elliptical tubes were Z=1.235, 1.471, 1.706, respectively. The other size details can be found from Figs. 2 and 3. In addition to the difference in the elliptical tube structures and a built-in turbulator between this paper and our previous paper [44], another crucial point is that only thermal efficiency was used to estimate the energy from quantity in our previous paper [44], but exergy efficiency was proposed to evaluate the energy from quality in this paper, which can guide us how to choose enhanced heat transfer technology from the quality of energy.

3. Data Processing

Heat power of DC power Q_j:

$$Q_j = UI \tag{1}$$

Effective heat power of DC power Q_{je}:

$$Q_{je} = UI - Q_{loss} \tag{2}$$

Specific heat and density of nanofluids [45]:

$$c_{pnf} = (1-\varphi)c_{pbf} + \varphi c_{pnp} \tag{3}$$

$$\rho_{nf} = (1-\varphi)\rho_{bf} + \varphi\rho_{np} \tag{4}$$

Equivalent relationship between the volume fraction and the mass concentration:

$$\varphi = \frac{1}{(1/\omega)(\rho_{np}/\rho_{nf})} \tag{5}$$

Absorbed heat of fluid Q_r:

$$Q_r = c_p q_m (T_{out} - T_{in}) \tag{6}$$

Heat exchange amount between tube and fluid Q:

$$Q = \frac{Q_{je} + Q_r}{2} \tag{7}$$

Temperature of the outer wall T_{wo}:

$$T_{wo} = \frac{\sum_{i=1}^{11} T_{wo}(i)}{11},\ (i = 1, 2, 3 \ldots 11) \tag{8}$$

Temperature of the inner wall T_{wi}:

$$T_{wi} = T_{wo} - \frac{Q\ln(r_{out}/r_{in})}{2\pi Lk} \tag{9}$$

Temperature of fluid T_f:

$$T_f = \frac{T_{in} + T_{out}}{2} \tag{10}$$

Convection heat transfer coefficient h_{nf}:

$$h_{nf} = \frac{Q}{\pi d_e L(T_{wi} - T_f)} \tag{11}$$

Nusselt number:

$$Nu = \frac{h_{nf} d_e}{\lambda_f} \tag{12}$$

Frictional resistance coefficient f:

$$f = \frac{2d_e}{\rho u^2} \cdot \frac{\Delta p}{\Delta l} \tag{13}$$

Reynolds number Re:

$$Re = \frac{\rho u d_e}{\mu_{nf}} \tag{14}$$

Thermal efficiency index η [46]:

$$\eta = \left(\frac{Nu}{Nu_{(bf+circular\ tube)}}\right) \Big/ \left(\frac{f}{f_{(bf+circular\ tube)}}\right)^{\frac{1}{3}} \tag{15}$$

Equation of the exergy efficiency plot [47]:

$$\ln\left(\frac{Nu_e}{Nu_0}\right)_{Re} = b_i + k_i \ln\left(\frac{f_e}{f_0}\right)_{Re} \tag{16}$$

where $b_P = \ln C_{Q,P}$, $b_{\Delta p} = \ln C_{Q,\Delta p}$, $b_V = \ln C_{Q,V}$, $-1 \le m_1 < 0$, $0 < m_2 < 1$.

4. Uncertainty Analysis

The uncertainty equations [48]:

$$\frac{\delta Nu}{Nu} = \sqrt{\left(\frac{\delta Q_f}{Q_f}\right)^2 + \left(\frac{\delta T}{T}\right)^2} \tag{17}$$

$$\frac{\delta f}{f} = \sqrt{\left(\frac{\delta p}{p}\right)^2 + \left(\frac{\delta L}{L}\right)^2 + \left(\frac{\delta q_m}{q_m}\right)^2} \tag{18}$$

Table 2. Experimental instrument and its uncertainty

Experimental instrument	Precision
DC power	1.0%
Thermocouple	1.0%
Pressure transmitter	0.5%
Vernier caliper	0.1%
Rotameter	1.06%

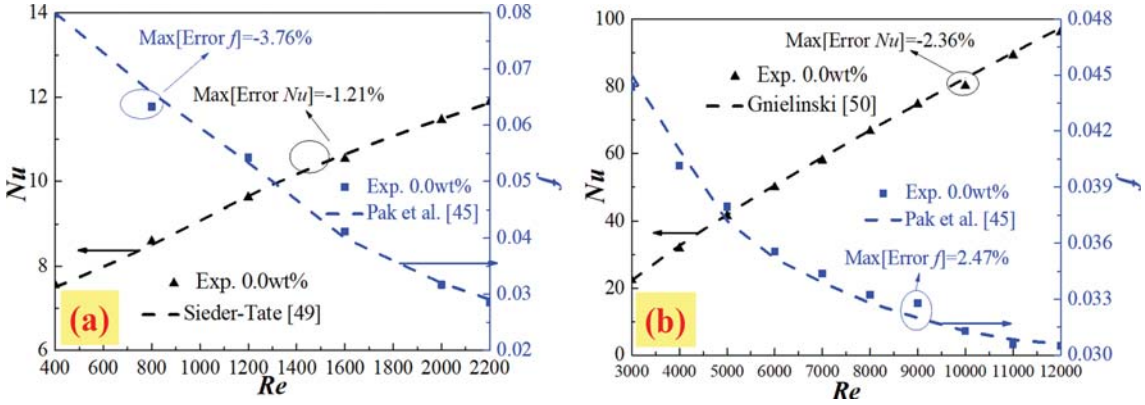

Fig. 4. Comparison between the results in this article and that of other published references, (a) laminar flow, (b) turbulent flow.

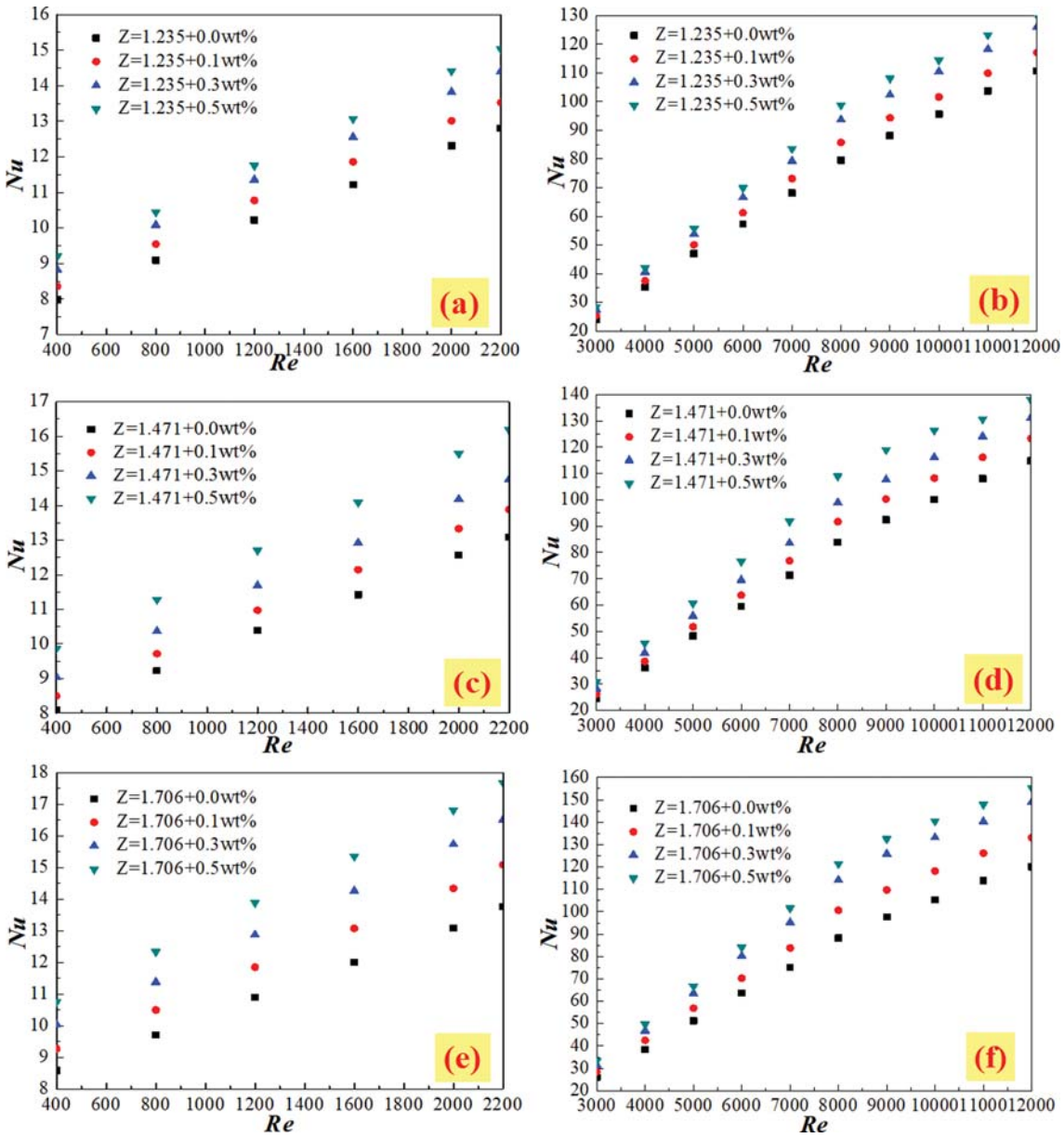

Fig. 5. Effects of nanoparticle concentration on Nusselt number of elliptical tubes with diverse axial ratios, Z=1.235: (a) laminar flow, (b) turbulent flow, Z=1.471: (c) laminar flow, (d) turbulent flow, Z=1.706: (e) laminar flow, (f) turbulent flow.

The precision of the experimental instrument (or equipment) in the experiment is presented in Table 2. Based on Eqs. (17) and (18), the indeterminacy of Nu and f was 1.41% and 1.18%, respectively. The result indicated that error was less than 3.0%, which can guarantee the reliability and accuracy of the experiment in this paper.

RESULTS AND DISCUSSION

1. Verification

The experiment was verified on the experimental system first. The thermal-hydraulic properties of water in a round tube were researched and a comparison was made with the published references [45,49,50]. The comparisons between the results in this article and that of published references are given in Fig. 4. It was found that the max error for Nu was 1.21% and 2.36% at laminar and turbulent flow, respectively, and the max error for f was 3.76% and 2.47% at laminar and turbulent flow, respectively. The errors were all small and capable of verifying the credibility of this system.

2. Elliptical Tubes without a Built-in Turbulator

2-1. Effects of Nanoparticle Concentration

The effects of nanoparticle concentration on the thermo-hydraulic properties are analyzed in the section. The effects of nanoparticle concentrations on Nu of elliptical tubes with various axial ratios (Z=1.235, 1.471, 1.706) are presented in Fig. 5. Results make clear that Nusselt number increases with the nanoparticle concentration. At laminar flow, nanofluids with ω=0.5 wt% can improve the thermal performance by 14.8%, 19.2%, 22.2% at best compared with water when Z=1.235, 1.471, 1.706, respectively. At turbulent

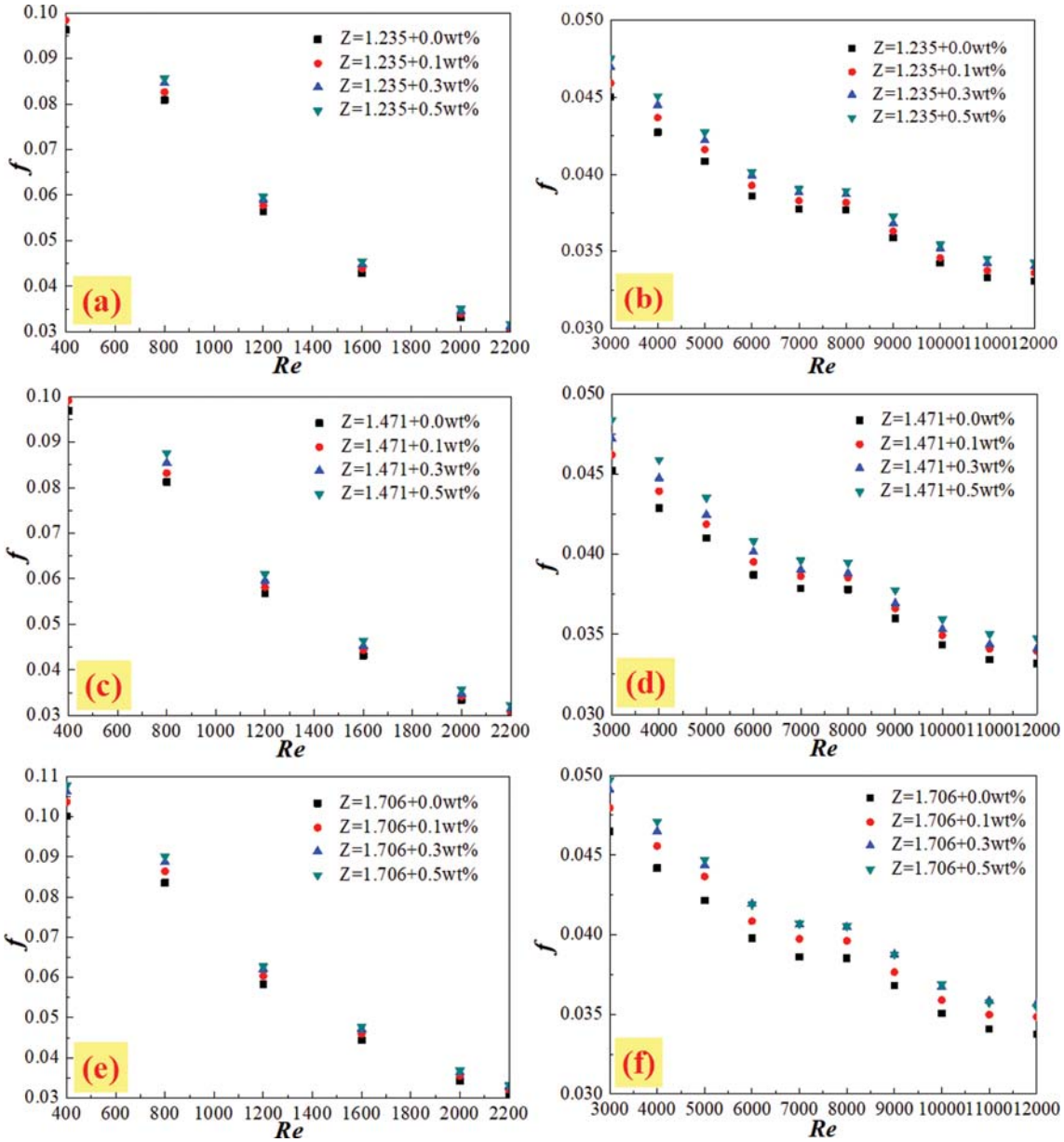

Fig. 6. Effects of nanoparticle concentration on resistance coefficient in elliptical tubes with diverse axial ratios, Z=1.235: (a) laminar flow, (b) turbulent flow, Z=1.471: (c) laminar flow, (d) turbulent flow, Z=1.706: (e) laminar flow, (f) turbulent flow.

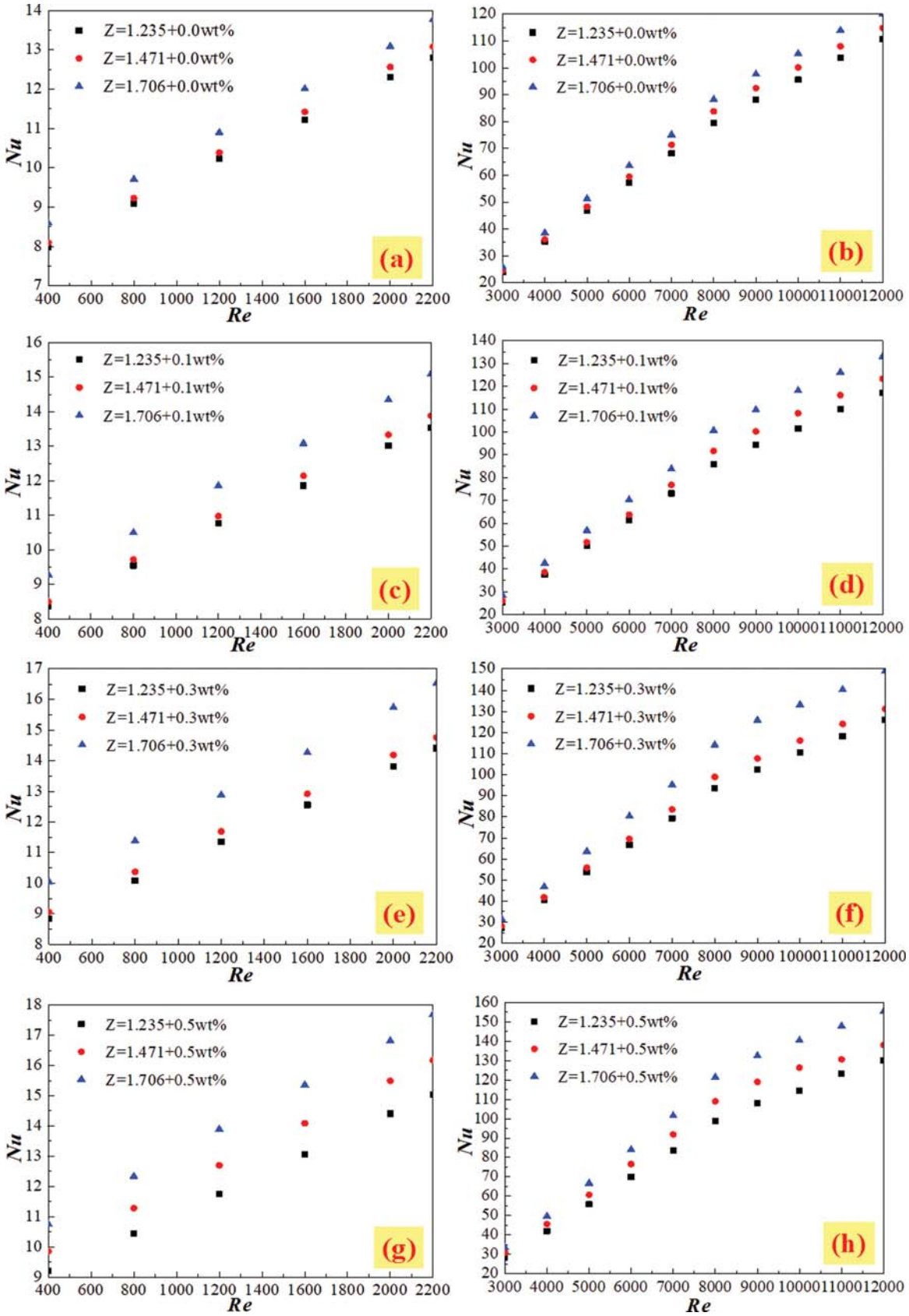

Fig. 7. Effects of axial ratios on Nusselt number of nanofluids with diverse nanoparticle concentrations, ω=0.0 wt%: (a) laminar flow, (b) turbulent flow, ω=0.1 wt%: (c) laminar flow, (d) turbulent flow, ω=0.3 wt%: (e) laminar flow, (f) turbulent flow, ω=0.5 wt%: (g) laminar flow, (h) turbulent flow.

flow, nanofluids with ω=0.5 wt% can strengthen the thermal performance by 19.4%, 23.1%, 27.3% at best compared with water when Z=1.235, 1.471, 1.706, respectively. One reason is that nanofluids have high heat conductivity, and another reason is that Brownian force shows the largest one among interaction forces (gravity and buoyancy force, drag force, interaction potential force, Brownian force), and can cause a large disturbance in the fluid [51].

Results also indicate that the increasing proportion at laminar flow is much smaller than that at turbulent flow. This can be interpreted that the laminar boundary layer at laminar flow is much thicker than that at turbulent flow, and heat conduction becomes the most critical influence on the laminar boundary layer; however, nanoparticle concentrations are very close, which results in a small increase ratio at laminar flow. When the flow enters into turbulent, the laminar boundary layer becomes thin and the influence of heat conduction decreases, but the increasing turbulence caused by Brownian force becomes the major factor which affects the increase ratio; therefore, the increase proportion of turbulent flow becomes much greater than that of laminar flow.

Along with the increase of nanoparticle concentration, apart from the improvement of thermal performance, the resistance coefficient also increases, which gives rise to the heat transfer system to consume additional energy to transport nanofluids. Therefore, the impact of nanoparticle concentration on coefficient of resistance in elliptical tubes with various axial ratios is also discussed in this section, which is shown in Fig. 6. Results show that the f has an increasing tendency with the increase of nanoparticle concentration. At laminar flow, nanofluids with ω=0.5 wt% can increase the f by 6.0%, 7.6%, 7.2% at greatest compared with water when Z=1.235, 1.471, 1.706, respectively. At turbulent flow, nanofluids with ω=0.5 wt% can increase the f by 5.2%, 6.6%, 6.5% at best compared with water when Z=1.235, 1.471, 1.706, respectively. This can be mainly interpreted by the Stokes force between nanoparticles and water molecules due to the diverse mass; when the nanoparticles are added into the base fluids, there is a difference in velocity between nanoparticles and water molecules. Hence, with the increase of nanoparticle concentration, the drag force can show an increasing trend, and a large drag force directly causes large viscosity and resistance coefficient. Results also present that the increase proportion of the f at laminar flow is slightly smaller than that at turbulent flow, and they differ very little from each other. This may be explained as follows: the drag force plays a more crucial role in the resistance coefficient compared with other factors, and the velocity difference between nanoparticles and water molecules at laminar flow is slightly smaller than that at turbulent flow, but they differ very little from each other.

2-2. Effects of Axial Ratio

The effects of the axial ratios of the elliptical tube on the thermo-hydraulic properties are analyzed in this section. Fig. 7 illustrates the influence of axial ratio on Nusselt numbers of nanofluids with various nanoparticle concentrations (ω=0.0 wt%, 0.1 wt%, 0.3 wt%, 0.5 wt%). Results indicate that Nu shows a growing tendency with the rise of the axial ratio. The elliptical tube with axial ratio Z=1.706 shows the largest thermal performance, and it can increase the Nusselt number by 7.1%, 10.3%, 12.8%, 15.4% at best compared with that with axial ratio Z=1.235 for nanofluids with ω=0.0 wt%, 0.1 wt%, 0.3 wt%, 0.5 wt% at laminar flow, respectively. It can increase the Nusselt number by 9.8%, 14.8%, 18.7%, 18.6% at best compared with that with axial ratio Z=1.235 for nanofluids with ω=0.0 wt%, 0.1 wt%, 0.3 wt%, 0.5 wt% at turbulent flow, respectively. This can be explained that the most inner side of the elliptical tube is much nearer to the center with the increase of axial ratio, then the velocity gradient becomes much larger, and the large velocity diminishes the thickness of the laminar boundary layer, which causes higher thermal performance. A large axial ratio of the elliptical tube is advantageous for enhancing heat transfer.

Another conclusion is also obtained that the increase proportion of Nusselt number at turbulent flow is higher than that at laminar flow. The reason is similar to that in the previous section. Nanoparticle concentrations are very close, which results in a small increase ratio at laminar flow. When the flow enters into the turbulent flow, Brownian force becomes the major factor that affects the increase ratio rather than thermal conductivity, and Brownian force increases with the increasing axial ratio; therefore, the increase ratio of turbulent flow becomes much greater than that of laminar flow.

Also, the effects of axial ratio on the resistance coefficients of nanofluids with various nanoparticle concentrations (ω=0.0 wt%, 0.1 wt%, 0.3 wt%, 0.5 wt%) are investigated in Fig. 8. Results indicate that the f has an upward tendency with the axial ratio. The elliptical tube with axial ratio Z=1.706 shows the largest resistance coefficient, and it can augment the resistance coefficient by 3.8%, 5.13%, 5.07%, 5.0% at best compared with that with axial ratio Z=1.235 for nanofluids with ω=0.0 wt%, 0.1 wt%, 0.3 wt%, 0.5 wt% at laminar flow or turbulent flow, respectively. According to above analysis, the velocity gradient becomes larger with the increase of axial ratio, and the velocity difference between nanoparticles and water molecules becomes larger. Hence, the drag force caused by the velocity difference shows an increasing trend with the axial ratio. Lastly, the large drag force causes a high resistance coefficient. Another conclusion is that the increase ratio of the f at laminar flow is almost identical with that at turbulence flow. This may be owing to the reasons that the structure of the elliptical tube has little impact on the resistance coefficient, and the nanoparticle concentration becomes the foremost factor.

3. Elliptical Tubes with a Built-in Turbulator

3-1. Effect of Nanoparticle Concentration

To augment the heat transfer further, a turbulator is put inside of the elliptical tubes. Impacts of nanoparticle concentrations on the Nu of various axial ratio elliptical tubes with a built-in turbulator are discussed, which is presented in Fig. 9. Conclusions show that the thermal properties also rise with the nanoparticle concentration, just like the elliptical tubes without a built-in turbulator. At laminar flow, nanofluids with ω=0.5 wt% can improve the thermal performance by 18.7%, 23.0%, 26.8% at best compared with water when Z=1.235, 1.471, 1.706, respectively. At turbulent flow, nanofluids with ω=0.5 wt% can improve the thermal performance by 24.5%, 26.2%, 33.8% at best compared with water when Z=1.235, 1.471, 1.706, respectively. The reason is similar to the elliptical tubes without a built-in turbulator (Fig. 5). Compared with nanofluids in elliptical tubes without a built-in turbulator at laminar and turbulent flow, nanofluids in elliptical tubes with a built-in turbulator

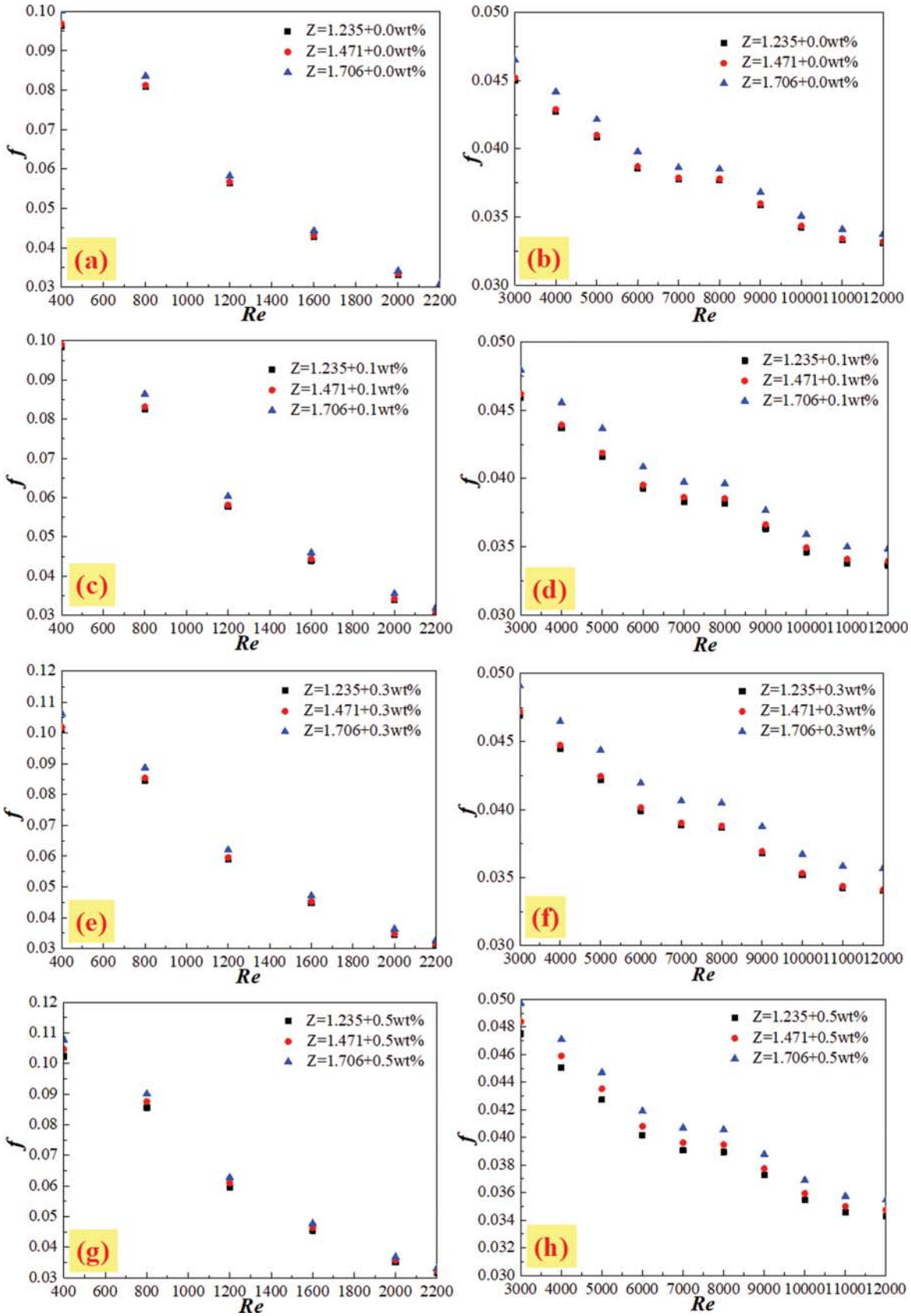

Fig. 8. Effects of axial ratios on resistance coefficients of nanofluids with diverse nanoparticle concentrations, ω=0.0%: (a) laminar flow, (b) turbulent flow, ω=0.1%: (c) laminar flow, (d) turbulent flow, ω=0.3%: (e) laminar flow, (f) turbulent flow, ω=0.5%: (g) laminar flow, (h) turbulent flow.

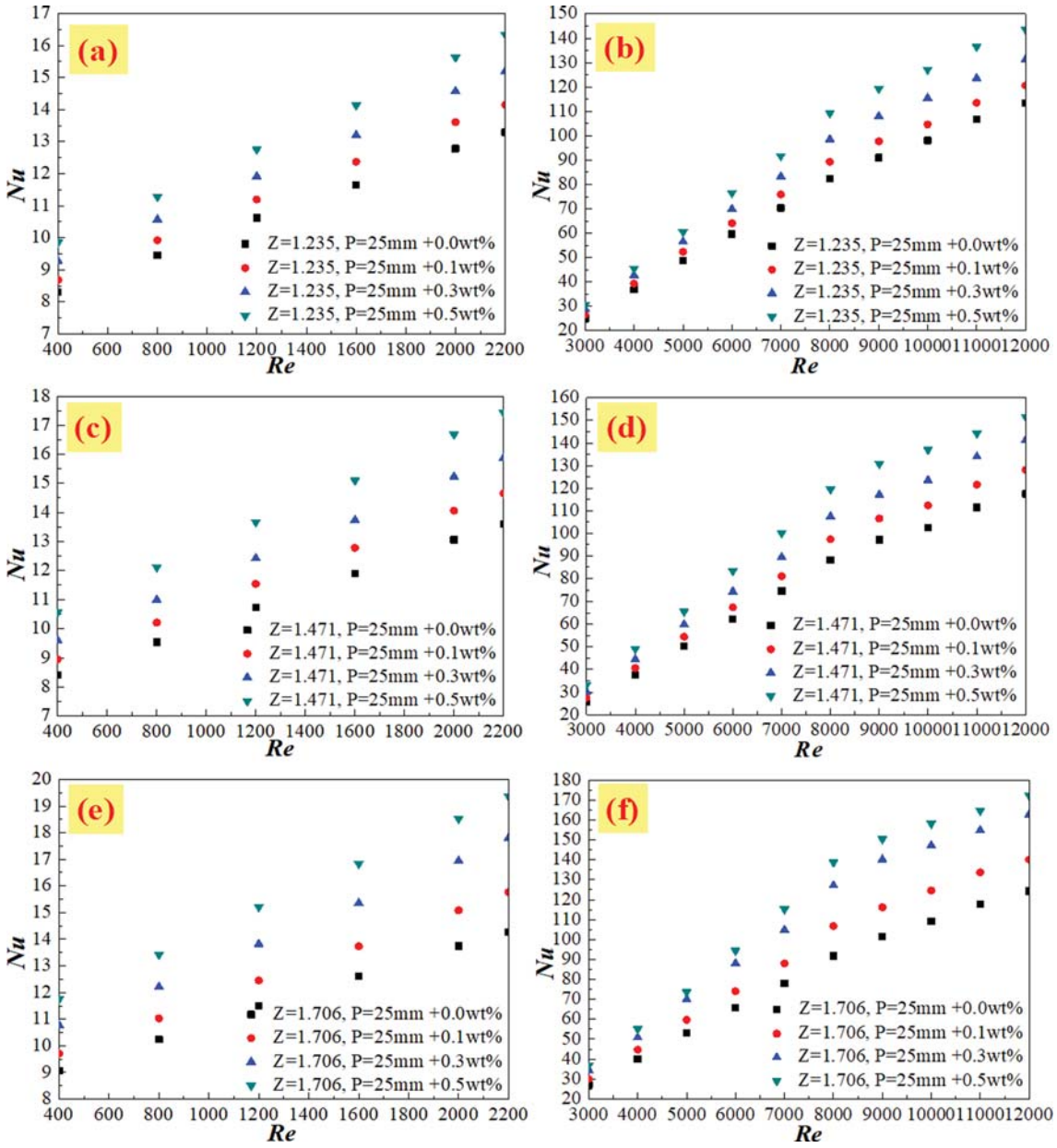

Fig. 9. Effects of nanoparticle concentration on Nusselt number of diverse axial ratio elliptical tubes with built-in turbulator, Z=1.235: (a) laminar flow, (b) turbulent flow, Z=1.471: (c) laminar flow, (d) turbulent flow, Z=1.706: (e) laminar flow, (f) turbulent flow.

can improve the thermal performance by 9.2% and 12.5% at best respectively, which can be interpreted by the insertion of the turbulator. On one hand, the effective flow area of the tube decreases and the average flow velocity in the elliptical tube increases. Meanwhile, nanofluids are forced to flow in spirals due to the turbulator. On the other hand, the shear stress at the wall is boosted and the disturbance caused by secondary flow is enhanced, and then the thickness of the laminar boundary layer is reduced, ultimately the heat transfer effect is improved.

Also, the impact of nanoparticle concentration on the f in various axial ratio elliptical tubes with a built-in turbulator was investigated, which is given in Fig. 10. Results illustrate that the f also increases with the nanoparticle concentration, just like the elliptical tubes without a built-in turbulator. At laminar flow, nanofluids with ω=0.5 wt% can enlarge the f by 6.4%, 7.2%, 8.0% at greatest compared with water when Z=1.235, 1.471, 1.706 respectively. At turbulent flow, nanofluids with ω=0.5 wt% can enhance the resistance coefficient by 6.3%, 7.4%, 8.3% at greatest compared with water when Z=1.235, 1.471, 1.706, respectively. Results also indicate that the increase proportion of the resistance coefficient at laminar flow is slightly less than that at turbulent flow and they are close to each other. The reason is similar to the elliptical tubes without a built-in turbulator (Fig. 6). Compared with nanofluids in elliptical tubes without a built-in turbulator, nanofluids in elliptical tubes with a built-in turbulator can enhance the resistance coefficient by 3.7% and 4.1% at laminar flow and turbulent flow at best, respec-

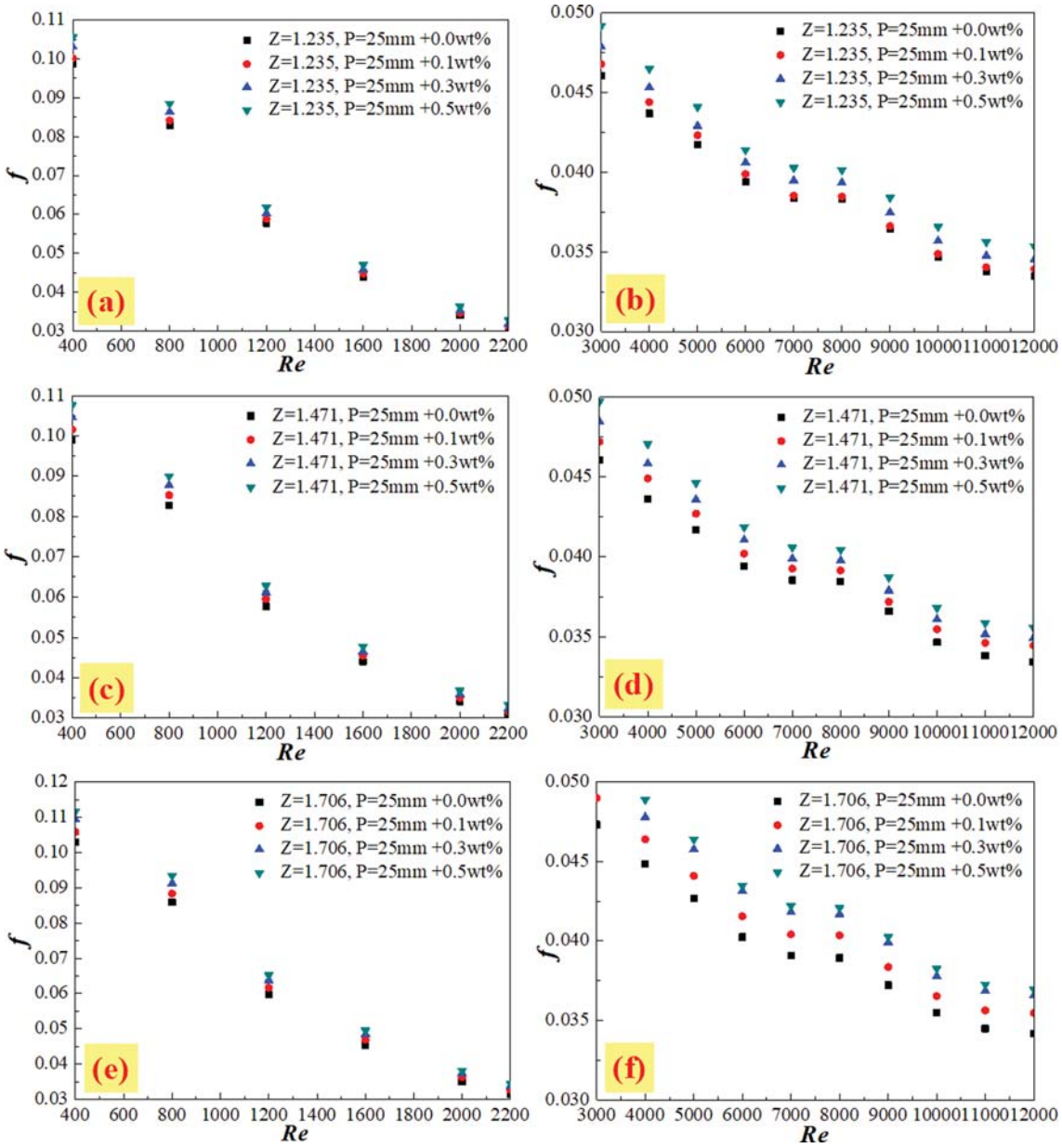

Fig. 10. Effects of nanoparticle concentration on resistance coefficient of diverse axial ratio elliptical tubes with built-in turbulator, Z=1.235: (a) laminar flow, (b) turbulent flow, Z=1.471: (c) laminar flow, (d) turbulent flow, Z=1.706: (e) laminar flow, (f) turbulent flow.

tively, which can be explained by the disturbance caused by the turbulator. The turbulator strengthens the mixing disturbance of the fluid, and also brings large friction between nanofluids and the wall surface. Hence, there will be a large pressure drop loss.

3-2. Effects of Axial Ratio

The effects of axial ratios on Nu of nanofluids with various nanoparticle concentrations in elliptical tubes with a built-in turbulator are illustrated in Fig. 11. It is indicated that Nusselt number displays an increasing tendency with the increase of axial ratio. The elliptical tube with axial ratio Z=1.706 shows the largest thermal performance, and it can increase the Nusselt number by 8.5%, 10.6%, 14.6%, 16.2% at best compared with that with axial ratio Z=1.235 for nanofluids with ω=0.0 wt%, 0.1 wt%, 0.3 wt%, 0.5 wt% at laminar flow, respectively. It can increase the Nusselt number by 10.2%, 16.3%, 23.0%, 21.3% at best compared with that with axial ratio Z=1.235 for nanofluids with ω=0.0 wt%, 0.1 wt%, 0.3 wt%, 0.5 wt% at turbulent flow, respectively. Another conclusion also is that the increase proportion of Nu at turbulent flow is greater than that at laminar flow. The reason is the same as the elliptical tube without a built-in turbulator. Compared with nanofluids in elliptical tubes without a built-in turbulator, nanofluids in elliptical tubes with a built-in turbulator can improve the thermal performance by 8.0% and 10.0% at laminar flow and turbulent flow at most, which can be also explained by the disturbance caused by the turbulator. The boundary layer of the fluids on the inner surface of the elliptical tube is destroyed and reduced owing to the distur-

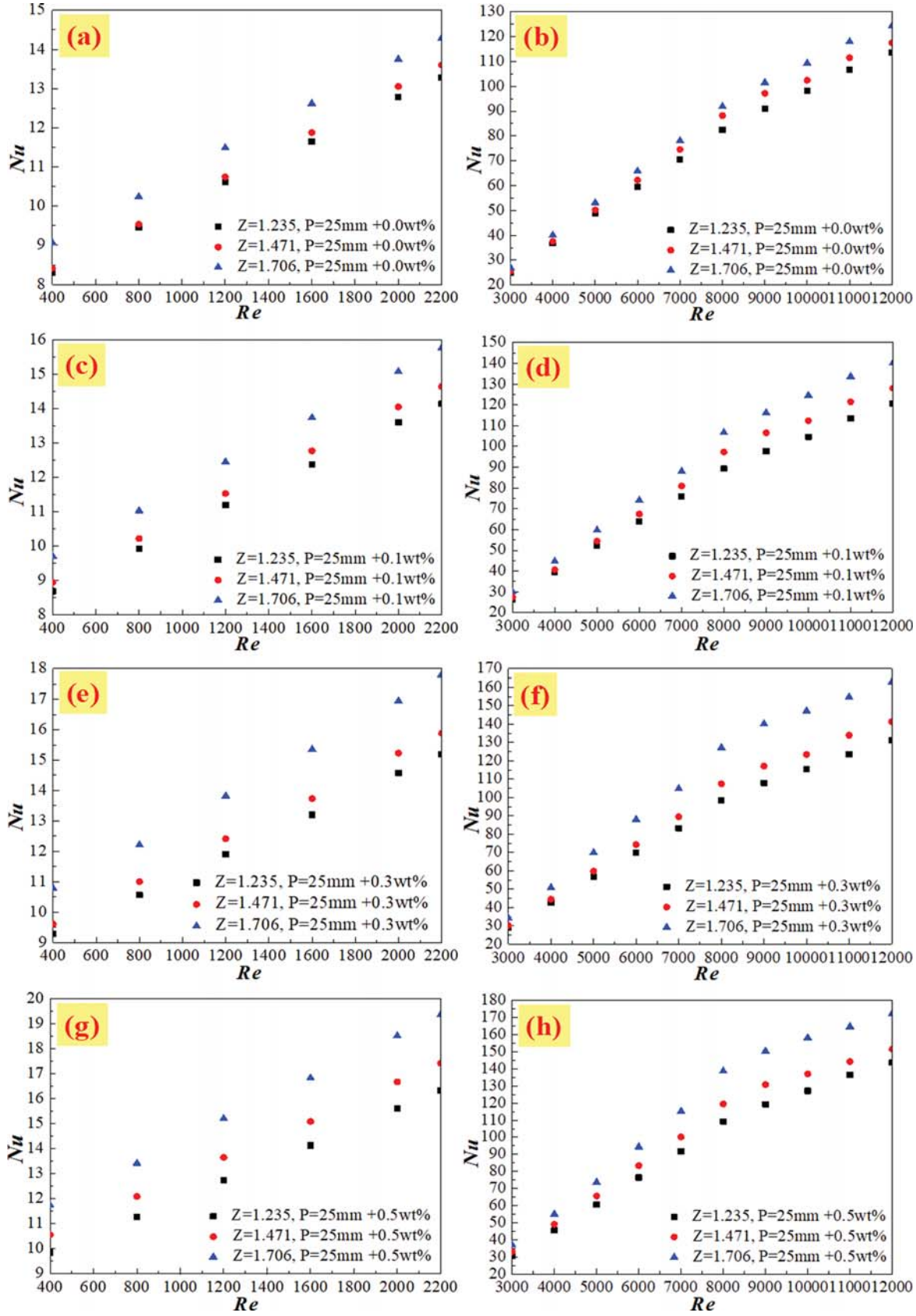

Fig. 11. Effects of axial ratios on Nusselt number of nanofluid in elliptical tubes with built-in turbulator, ω=0.0%: (a) laminar flow, (b) turbulent flow, ω=0.1%: (c) laminar flow, (d) turbulent flow, ω=0.3%: (e) laminar flow, (f) turbulent flow, ω=0.5%: (g) laminar flow, (h) turbulent flow.

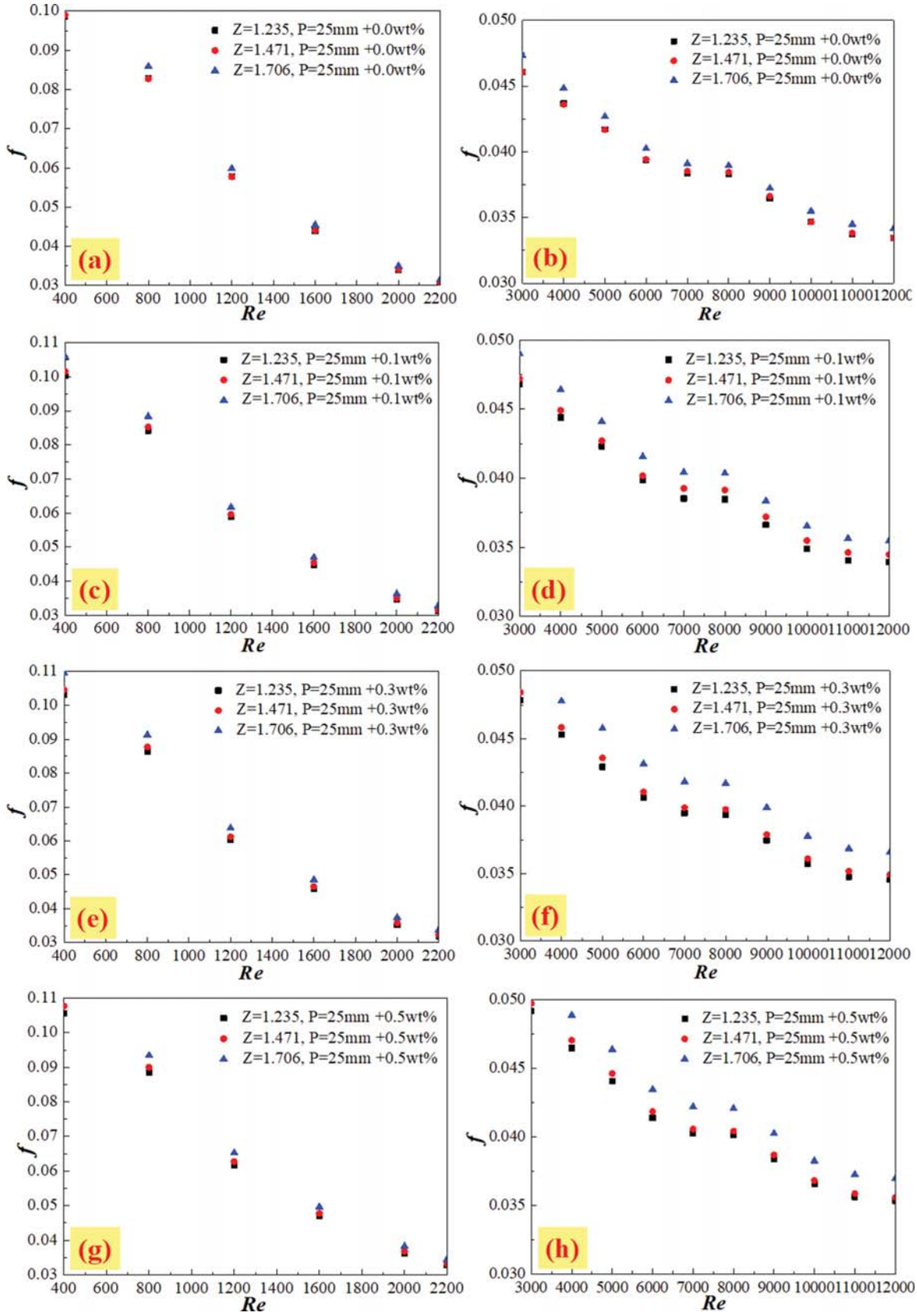

Fig. 12. Effects of axial ratios on resistance coefficient of nanofluid in elliptical tubes with built-in turbulator, ω=0.0%: (a) laminar flow, (b) turbulent flow, ω=0.1%: (c) laminar flow, (d) turbulent flow, ω=0.3%: (e) laminar flow, (f) turbulent flow, ω=0.5%: (g) laminar flow, (h) turbulent flow.

bance caused by the turbulator; lastly, the intensity of the heat transfer is increased.

The effects of axial ratio on f of nanofluids with various nanoparticle concentrations in elliptical tubes with a built-in turbulator are shown in Fig. 12. Results indicate that the f has an increase tendency with the increase of axial ratio. It can be found that the elliptical tube with axial ratio Z=1.706 shows the largest resistance coefficient, and it can all increase the resistance coefficient by 4.2%, 5.3%, 6.1%, 5.5% at best compared with that with axial ratio Z=1.235 for nanofluids with ω=0.0 wt%, 0.1 wt%, 0.3 wt%, 0.5 wt% at laminar flow or turbulent flow, respectively. An identical increase proportion of resistance coefficient is shown between laminar flow and turbulent flow. The reason is the same as with the elliptical tube without a built-in turbulator.

4. Thermal Efficiency

Increasing nanoparticle concentration and axial ratio can dramatically promote the heat transfer, but also contribute to the increase in resistance coefficient. A large resistance coefficient is not advantageous for enhancing heat transfer. Therefore, it is necessary to assess thermo-hydraulic performance comprehensively. Firstly, a thermal efficiency evaluation on the thermo-hydraulic characteristics is conducted from the quantity, whose outcomes are presented in Fig. 13. The thermal efficiency index η firstly shows an increase trend with the increasing Re and then diminishes. There exists a Re_c=8,000 which corresponds to the maximum value of the thermal efficiency index. Results also indicate that the thermal efficiency index increases with the nanoparticle concentration and axial ratio. Nanofluids with ω=0.5% in the elliptical tube without and with a turbulator at Re_c=8,000 all show the biggest thermal efficiency index, which can reach 1.35 and 1.47, respectively. This is because with the growth of Reynolds number, the augment ratio of heat transmission (Nu) is larger than that of the resistance coefficient as the Re is smaller than Re_c=8,000; however, after Re_c=8,000, the increase ratio of resistance coefficient assumes a major role. Hence, a Reynolds number (Re_c=8,000) that corresponds to the highest thermal efficiency index η appears. In terms of thermal efficiency, it is best to choose the Reynolds number (Re_c=8,000) as the most suitable working condition in the elliptical tubes with a built-in turbulator.

5. Exergy Efficiency

In addition to the thermal efficiency, exergy efficiency analysis was conducted on the heat transfer system from the viewpoint of quality instead of quantity. An exergy efficiency plot based on Eq. (16) was used to investigate the thermal and hydraulic characteristics (see Fig. 14). The plot is separated into four areas (area I- area IV) by three solid lines which are the identical mass flow rate condition, the identical pump power condition, the identical pressure drop condition from top to bottom. Data in area I means it is capa-

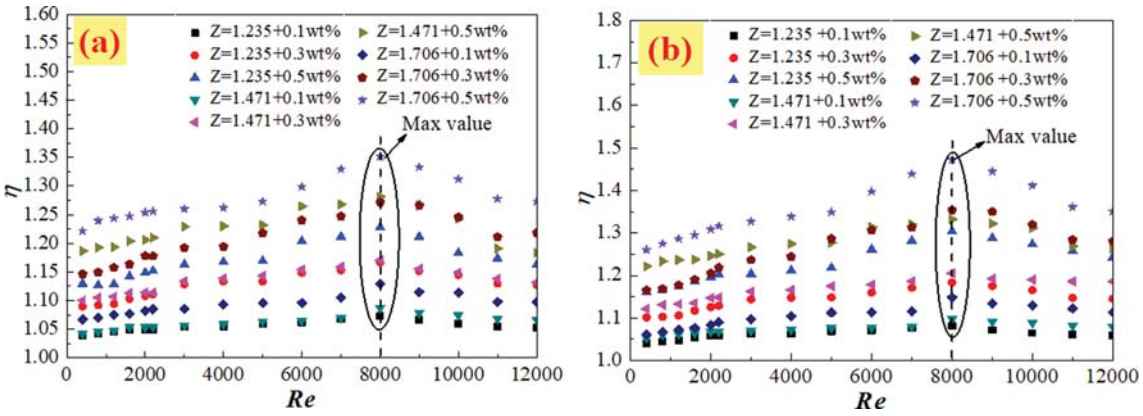

Fig. 13. Thermal efficiency analysis of thermo-hydraulic performance, (a) without turbulator, (b) with turbulator, p=25 mm.

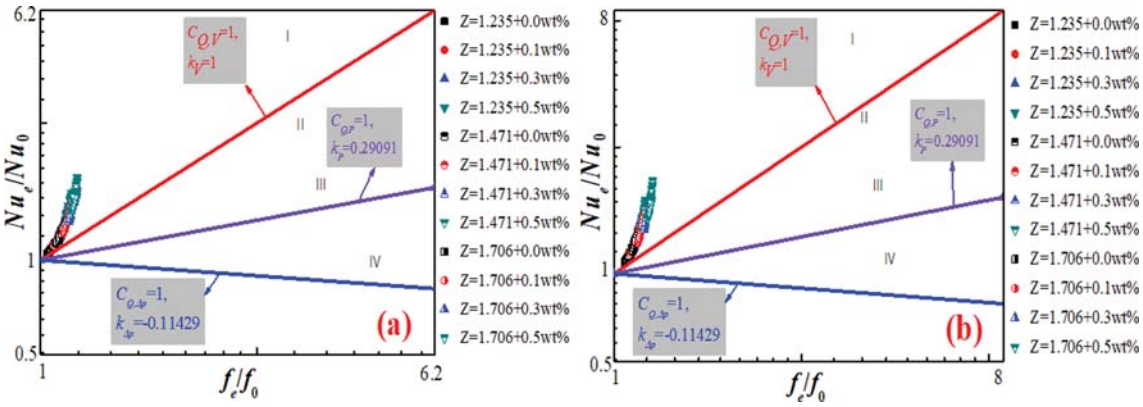

Fig. 14. Exergy efficiency analysis of thermo-hydraulic performance, (a) without turbulator, (b) with turbulator, p=25 mm.

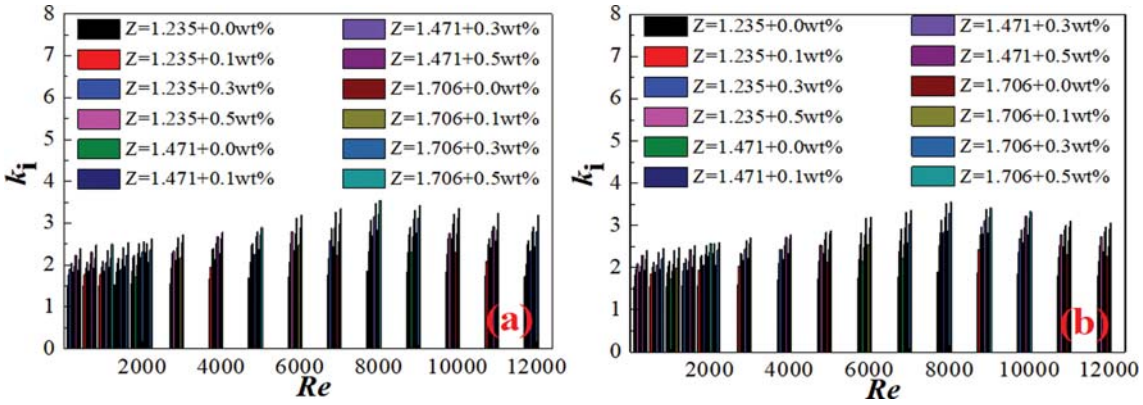

Fig. 15. The slope of experimental data in Fig. 14, (a) without turbulator, (b) with turbulator, p=25 mm.

ble of boosting the heat transfer under the condition of the identical mass flow rate. Data in area II means it can enhance the heat transfer under the identical requirement of pump power but deteriorates under the identical requirement of mass flow rate. Data in area III means it can evidently promote the heat transfer under the identical requirement of pressure drop but deteriorates under the identical requirement of pump power. Data in area IV means it can deteriorate under the identical requirement of pressure drop. Hence, area I indicates the best thermal characteristic; next is area II and area III, and area IV shows the weakest thermal characteristic. In Fig. 14 that all the data is located in area I, which means all the working conditions and enhancement techniques adopted in this paper (nanofluids instead of common fluid, elliptical tube instead of smooth tube) can clearly contribute to the improvement of heat transfer at the expense of barely a rise in f and have high exergy efficiency.

Although all the data is located in area I, in order to analyze them further, the slopes of experimental data in Fig. 14 are investigated and shown in Fig. 15. As we know from the analysis of Fig. 14, the higher the slope of the data is, the better is the exergy efficiency of the data. As can be seen from Fig. 15, the highest exergy efficiency manifests at Re=8,000, which provides us a principle to choose the working condition from the point of energy quality.

CONCLUSIONS

An experimental study was done to investigate the effects of axial ratio on thermo-hydraulic characteristics of nanofluids in elliptical tubes with a built-in turbulator on the basis of thermal and exergy efficiency. Some major conclusions are presented below:

(1) Thermal property of nanofluids was improved by the nanoparticle concentration, nanofluids with ω=0.5% showed the highest thermal property and could improve it by 27.3% and 33.8% at best in elliptical tubes without and with a built-in turbulator, respectively.

(2) Thermal property of nanofluids increased with the axial ratio of the elliptical tube. The elliptical tube with axial ratio Z=1.706 showed the largest thermal performance, and it, without and with a built-in turbulator, can promote the Nusselt number by 15.4% and 18.6% at best compared with that with an axial ratio Z=1.235, respectively.

(3) Resistance coefficient showed a little increasing trend with the increase of nanoparticle concentration and axial ratio. Compared with water at laminar and turbulent flow, nanofluids with ω=0.5 wt% in the elliptical tube without and with a built-in turbulator could augment the resistance coefficient by 6.5% and 8.3% at best, respectively.

(4) The thermal efficiency index first showed an increasing trend with the increasing Re and then diminished. There existed a Re_c= 8,000 which corresponds to the maximum value of the thermal efficiency index. Nanofluids with ω=0.5% at Re_c=8,000 showed the biggest thermal efficiency index which can reach 1.35 and 1.47, respectively.

(5) The working conditions and enhancement techniques adopted in this paper can clearly contribute to the improvement of heat transfer at the expense of little augment in f under the identical mass flow rate and show high exergy efficiency. The highest number appears at Re=8,000.

ACKNOWLEDGEMENTS

This work is financially supported by Natural Science Foundation of Jiangsu Province, China (Grant No. BK20181359).

NOMENCLATURE

a : radius of the long axis [mm]
b : radius of the short axis [mm]
c_p : heat volume of fluid [J·kg^{-1}·K^{-1}]
d_e : equivalent diameter [m]
f : frictional resistance coefficient
h : convective heat transfer coefficient [W·m^{-2}·K^{-1}]
H : width of turbulator [mm]
I : electric current [A]
k : thermal conductivity of tube [W·m^{-1}·K^{-1}]
L : length [m]
Nu : Nusselt number
P : element length of turbulator [mm]
$\Delta p/\Delta l$: pressure drop per unit length [Pa·m^{-1}]
Q : heat exchange amount [J]

Q_j : heating power of DC power [J]
Q_{je} : effective heating power of DC power [J]
Q_{loss} : heat loss [J]
Q_r : heat absorbed by nanofluids [J]
q_m : mass flow rate [kg·s^{-1}]
U : voltage [V]
r : radius [m]
Re : Reynolds number
T : temperature [K]
u : velocity [m·s^{-1}]
Z : axial ratios

Greek Symbols

δ : thickness [m]
η : thermal efficiency index
λ_f : thermal conductivity of fluid [W·m^{-1}·K^{-1}]
μ_{nf} : dynamic viscosity [Pa·s]
ρ : density of fluid [kg·m^{-3}]
ω : mass fraction [%]

Subscripts

bf : base fluid
in : import
nf : nanofluids
out : outport
w : wall

REFERENCES

1. X. Wang, Y. Yan, X. Meng and G. Chen, *Appl. Therm. Eng.*, **157**, 113761 (2019).
2. X. Wang, X. Gao, K. Bao, C. Hua, X. Han and G. Chen, *J. Therm. Sci.*, **28**(2), 246 (2019).
3. A. Alirezaie, M. H. Hajmohammad, M. R. H. Ahangar and M. H. Esfe, *Appl. Therm. Eng.*, **128**, 373 (2018).
4. Y. S. Daniel, Z. A. Aziz, Z. Ismail, A. Bahar and F. Salah, *Korean J. Chem. Eng.*, **36**, 1021 (2019).
5. X. Liu and Y. Xuan, *Nanoscale*, **9**, 14854 (2017).
6. X. Liu and Y. Xuan, *Sol. Energy*, **146**, 503 (2017).
7. A. Asadi, M. Asadi, A. Rezaniakolaei, L. A. Rosendahl, M. Afrand and S. Wongwises, *Int. J. Heat Mass Transf.*, **117**, 474 (2018).
8. P. Samira, Z. H. Saeed, S. Motahare and K. Mostafa, *Korean J. Chem. Eng.*, **32**, 609 (2015).
9. M. Nasiri, S. G. Etemad and R. Bagheri, *Korean J. Chem. Eng.*, **28**, 2230 (2011).
10. M. A. Sheremet, I. Pop and O. Mahian, *Int. J. Heat Mass Transf.*, **116**, 751 (2018).
11. M. S. Astanina, M. A. Sheremet, H. F. Oztop and N. Abu-Hamdeh, *Int. J. Heat Mass Transf.*, **118**, 527 (2018).
12. I. V. Miroshnichenko, M. A. Sheremet, H. F. Oztop and N. Abu-Hamdeh, *Int. J. Heat Mass Transf.*, **125**, 648 (2018).
13. S. A. Mikhailenko, M. A. Sheremet, H. F. Oztop and N. Abu-Hamdeh, *Int. J. Mech. Sci.*, **156**, 137 (2019).
14. F. Selimefendigil and H. F. Öztop, *Int. J. Heat Mass Transf.*, **129**, 265 (2019).
15. M. Izadi, A. Behzadmehr and M. M. Shahmardan, *Korean J. Chem. Eng.*, **31**, 12 (2014).
16. H. Sajjadi, A. A. Delouei, M. Izadi and R. Mohebbi, *Int. J. Heat Mass Transf.*, **132**, 1087 (2019).
17. R. Mohebbi, M. Izadi, H. Sajjadi, A. A. Delouei and M. A. Sheremet, *Physica A*, **526**, 120831 (2019).
18. Y. Hu, Y. He, H. Gao and Z. Zhang, *Appl. Therm. Eng.*, **155**, 650 (2019).
19. Z. Li, A. Shahsavar, A. A. Al-Rashed and P. Talebizadehsardari, *Appl. Therm. Eng.*, **167**, 114777 (2020).
20. X. Ma, M. Sheikholeslami, M. Jafaryar, A. Shafee, T. Nguyen-Thoi and Z. Li, *J. Clean. Prod.*, **245**, 118888 (2018).
21. Z. Li, M. Sheikholeslami, M. Ayani, M. Shamlooei, A. Shafee, M. Waly and I. Tlili, *Physica A*, **524**, 540 (2019).
22. M. Sheikholeslami, A. Arabkoohsar, I. Khand, A. Shafee and Z. Li, *J. Clean. Prod.*, **221**, 885 (2019).
23. Z. Li, M. Sheikholeslami, A. J. Chamkha, Z. A. Raizah and S. Saleem, *Comput. Method. Appl. Mech. Eng.*, **338**, 618 (2018).
24. M. Sheikholeslami, M. Jafaryar, D. D. Ganji and Z. Li, *J. Mol. Liq.*, **262**, 104 (2018).
25. M. Sheikholeslami, M. Jafaryar and Z. Li, *Int. J. Heat Mass Transf.*, **124**, 980 (2018).
26. A. A. Al-Rashed, A. Shahsavar, S. Entezari, M. A. Moghimi, S. A. Adio and T. K. Nguyen, *Appl. Therm. Eng.*, **155**, 247 (2019).
27. A. A. Al-Rashed, R. Ranjbarzadeh, S. Aghakhani, M. Soltanimehr, M. Afrand and T. K. Nguyen, *Physica A*, **521**, 724 (2019).
28. J. Alsarraf, A. Moradikazerouni, A. Shahsavar, M. Afrand, H. Salehipour and M. D. Tran, *Physica A*, **520**, 275 (2019).
29. M. Nojoomizadeh, A. Karimipour, M. Firouzi and M. Afrand, *Int. J. Heat Mass Transf.*, **119**, 891 (2018).
30. P. Naphon, L. Nakharintr and S. Wiriyasart, *Int. J. Heat Mass Transf.*, **126**, 924 (2018).
31. M. U. Sajid and H. M. Ali, *Renew. Sust. Energy Rev.*, **103**, 556 (2019).
32. M. M. Sarafraz, V. Nikkhah, M. Nakhjavani and A. Arya, *Exp. Therm. Fluid Sci.*, **91**, 509 (2018).
33. M. M. Sarafraz, H. Arya and M. Arjomandi, *J. Mol. Liq.*, **263**, 382 (2018).
34. M. M. Sarafraz, M. R. Safaei, Z. Tian, M. Goodarzi, E. P. Bandarra Filho and M. Arjomandi, *Energies*, **12**, 1929 (2019).
35. M. Nasiri, S. G. Etemad and R. Bagheri, *Korean J. Chem. Eng.*, **28**, 2230 (2011).
36. S. Kim, H. Yoo and C. Kim, *Korean J. Chem. Eng.*, **29**, 1321 (2012).
37. R. Mohebbi, M. Izadi, A. A. Delouei and H. Sajjadi, *J. Therm. Anal. Calorim.*, **135**, 3029 (2018).
38. B. Sun, A. Yang and D. Yang, *Int. J. Heat Mass Transf.*, **107**, 712 (2017).
39. A. Karimi, A. A. Al-Rashed, M. Afrand, O. Mahian, S. Wongwises and A. Shahsavar, *Int. J. Mech. Sci.*, **156**, 397 (2019).
40. P. Naphon and S. Wiriyasart, *Int. J. Heat Mass Transf.*, **118**, 297 (2018).
41. P. Naphon and S. Wiriyasart, *Int. J. Heat Mass Transf.*, **125**, 1054 (2018).
42. P. Naphon, S. Wiriyasart and T. Arisariyawong, *Int. J. Heat Mass Transf.*, **118**, 1152 (2018).
43. C. Qi, M. Liu, G. Wang, Y. Pan and L. Liang, *Chin. J. Chem. Eng.*, **26**, 2420 (2018).
44. C. Qi, L. Yang, T. Chen and Z. Rao, *Appl. Therm. Eng.*, **129**, 1315

(2018).
45. B. C. Pak and Y. I. Cho, *Exp. Heat. Transf.*, **11**, 151 (1998).
46. C. Qi, Y. L. Wan, C. Y. Li, D. T. Han and Z. H. Rao, *Int. J. Heat Mass Transf.*, **115**, 1072 (2017).
47. C. Qi, G. Wang, Y. Yan, S. Mei and T. Luo, *Energy Convers. Manage.*, **166**, 744 (2018).
48. S. J. Kline, *Mech. Eng.*, **75**, 3 (1953).
49. E. N. Sieder and G. E. Tate, *Ind. Eng. Chem.*, **28**, 1429 (1936).
50. V. Gnielinski, *Int. Chem. Eng.*, **16**, 359 (1976).
51. C. Qi, L. Liang and Z. Rao, *Int. J. Heat Mass Transf.*, **94**, 316 (2016).